Odin/SMR

Algorithm Theoretical Basis Document: Level 1 Processing

Author(s): Bengt Rydberg, Patrick Eriksson, Joonas Kiviranta, Andreas Skyman, and Donal Murtagh

Contact: Bengt Rydberg <bengt.rydberg@molflow.com>

Version: 0.2

Date: 2016-01-06

Chalmers University of Technology
Department of Earth and Space Sciences

Contents

Introduction

Aim and scope of this document

The sub-millimetre radiometer (SMR) onboard the Odin satellite performs limb sounding measurements of the atmosphere. The basic output of Odin/SMR is spectra in different frequency bands, mainly within the $486 - 504\,\mathrm{GHz}$ and $541 - 581\,\mathrm{GHz}$ region. After calibration, a group of such spectra can be used to retrieve profiles of e.g. O_3, ClO, N_2O, HNO_3, H_2O, CO, and isotopologues of H_2O, and O_3, which are species that are of interest for studying stratospheric and mesospheric chemistry and dynamics.

The processing of data from basic instrumental data to the desired species concentration product involves a number of steps. It is standard practise to divide data products into different levels, such as:

- Level0 data: time tagged and sorted science and house-keeping data as well as orbit and pointing data in separate files

- Level1B data: groups of spectra, calibrated both in intensity and frequency. Pointing and instruments settings included.

- Level2 data: extracted geophysical data (i.e. geolocated profile of ozone concentration) from observed spectra

The aim of this document is to review and describe basic data (Level0) from Odin/SMR and the algorithms used to to processes Level0 data into gelocated and calibrated groups of spectra (scans), which is refered to as Level1B data. The aim is also to describe the Level1B data format and the quality of the data.

This document is organised as follows: Odin/SMR observations and measurement modes are described in Chapter 1. The calibration procedure is presented in Chapter 2, and the Level1B data format, including description of quality flags, is described in Chapter 3. Finally, Chapter 4 gives a summary with focus on the most important points to correctly understand the Odin/SMR Level1B data.

Odin

The Odin satellite was launched on 2001-02-20 into a sun-synchronous 18:00 hour ascending node orbit, carrying two co-aligned limb sounding instruments: OSIRIS (optical spectrograph and infrared imaging system) and SMR (sub-millimetre radiometer). Originally, Odin was used for both atmospheric and astronomical observations, however, since 2007 its only active mission is its aeronomy. Odin is a Swedish-led project in cooperation with Canada, France and Finland. Both of Odin's instruments are still functional, and the present operation of the satellite is partially performed as an ESA third party mission.

Table 1.1: Odin/SMR frontend frequency specification.

Frontend	Tuning range [GHz]
549 A1	541–558
495 A2	486–504
555 B2	547–564
572 B1	563–581
119 C	118.75

Table 1.2: Odin/SMR backend frequency specification.

Backend	Bandwidth [MHz]	Channel spacing [MHz]
AOS	1050	0.61
AC1/AC2	800	1.0
	400	0.5
	200	0.25
	100	0.125

Odin passes the ground station at Esrange about 14 times each day and raw science and house-keeping data are downloaded at Esrange and transferred to a data archive housed by the Parallel Data Centre (PDC) at the Royal Institute of Technology (KTH) in Stockholm.

The SMR instrument

The Odin/SMR package is highly tunable and flexible (Frisk et al., 2003). Odin/SMR is equipped with one mm and four sub-mm receivers. The four main sub-mm receiver chains can be tuned to cover frequencies in the ranges $486 - 504$ GHz and $541 - 581$ GHz. Table 1.1 lists the receivers single sideband (SSB) tuning ranges. Martin–Pulpett interferometers are employed to provide SSB filtering (with a nominal sideband suppression better than 19 dB across the image band) and injection into the Schottky mixers. The local oscillators are varactor-tuned Gunn diodes followed by doubler and tripler stages. The mixers and IF amplifiers are inside a cryostat and cooled to approximately 130 K by a 80 K Stirling cycle cooler. The receiver noise temperatures are around 3000 K for the sub-millimetre channels and 600 K for the millimetre channel.

The receivers form two groups, A1+A2 and B1+B2+C, in which each group shares a common path through the beam optics (Figure 1.1). The main observing mode is by switching against the cold sky, between the main beam and an unfocused sky beam. In switching mode, one group will receive its signal via the main beam while the other sees the reference signal, and vice versa. The two auto-correlators (ACs) of Odin/SMR can be coupled to any of the front-ends and each use up to 8 x 112 MHz bands. Eight correlator ships provides 96 lags each. The center IF (intermediate frequency) of each sub-band is tuneable within a 500 MHz wide band in 1 MHz steps. The channel spacing ranges from 125 KHz in 1 band mode to 1 MHz in 8 band mode (Table 1.2). Odin/SMR can be tuned to cover a wide frequency range, but the maximum total instantaneous bandwidth is only 1.6 GHz. In the configuration applied for atmospheric sounding, the channels of the ACs have a spacing of 1 MHz. To cover all molecular transitions of interest, a number of "observation modes" have been defined. Each observation mode makes use of two or three frequency bands. Definition of frequency modes are found in Tables A.1, A.2, and A.3, in Appendix A.

Odin/SMR has also a receiver chain around the 118 GHz oxygen transition which was
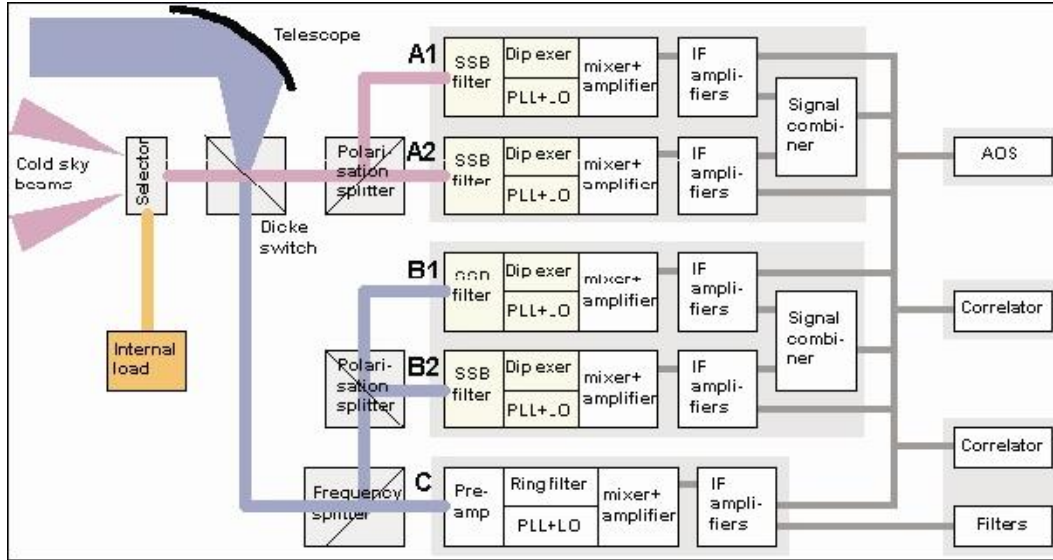
Chalmers University of Technology
Dept. of Earth and Space Sciences

2

Odin SMR
L1 Rev TN

Figure 1.1: Odin/SMR block diagram.

Table 1.3: Main scanning modes.

Scanning mode	Scanning range [km]
Stratospheric scan	7–72
Stratospheric/mesospheric scan	7–110
Summer mesospheric scan	60–100

heavily used during Odin's astronomy mission. For the atmospheric mission, this front-end was planned to be used for retrieving temperature profiles, but a technical problem (drifting LO frequency) and the fact that the analysis requires treatment of Zeeman splitting have given these data low priority.

The main reflector of Odin/SMR has a diameter of 1.1 m, giving a vertical resolution at the tangent point of about 2 km. Vertical scanning is achieved by a rotation of the satellite platform, by an advanced attitude control system (ACS). The ACS uses star trackers as the main sensors with backup from gyros, magnetometers, and Sun sensors. Reaction wheels and magnetic coils serve as actuators. The ACS pointing accuracy in limb-scanning mode is $5'$ in real time knowledge, and better than $1'$ in reconstructed knowledge (which translates to a $\sim$800 m vertical accuracy in tangent point). Measurements are generally performed along the orbit plane, providing a latitude coverage between 82.5°S and 82.5°N. Since the end of 2004 Odin also points off-track during certain periods, e.g. during the austral summer season, allowing the latitudinal coverage to be extended towards the poles.

Measurement sequence

The vertical scanning of Odin/SMR's line of sight is achieved by rotation of the platform with a rate matching a vertical speed of the tangent altitude of 750 m/s. Measurements are performed during both upward and downward scanning. The lower end of the scan is typically at about 7 km, and the upper end varies between 70 and 110 km depending on the observation mode (see Table 1.3).

For calibration purposes, Odin/SMR performs aeronomy observation in a switching mode, i.e. switching between the main beam and an unfocused sky beam of 4.4° FWHM

at all wavelengths. This is done by means of a chopper wheel. An internal selection mirror can choose between two possible directions of the sky beam, separated by 28°. The separation from the main beam amounts to 42°. The selection mirror may also direct the beam towards an internal load at ambient temperature (approximately 285 K), made of carbon loaded polyethylene tiles, optimised for reflecting less than -30 dB at 500 GHz.

Further reading

Murtagh et al. (2002) give an overview of the Odin aeronomy mission, as well as the general technical details of Odin/SMR. Frisk et al. (2003) give a description of the technical details of Odin/SMR.

Calibration procedure

Processing pipeline

Raw science and house-keeping data are downloaded at Esrange and transferred to a data archive housed by the Parallel Data Centre (PDC) at the Royal Institute of Technology (KTH) in Stockholm. The data processing for the calibration Odin/SMR measurements is performed at the Dept. of Earth and Space Sciences at Chalmers University of Technology (Chalmers) in Gothenburg. A file system at Chalmers is synchronized with the Level0-file archive at KTH. The KTH archive also contains files with reconstructed attitude information. Science and house-keeping data within those files are imported into Level0 tables of an Odin calibration database. Dedicated algorithms to process and combine new Level0 to Level1B data are executed on a regular basis and are described in this chapter. Level1B data are stored in tables of the Odin calibration database. Chapter 3 describes its format and how to access the Level1B data.

Radiometric calibration algorithm

Auto-correlator data

Data from the ACs must be transformed to spectra in the frequency domain prior to the radiometric calibration. This preparation of AC data basically involves a quantisation correction and the application of a Fourier transform. In the spectrometer hardware, the input signal is quantized into three levels: high positive, high negative, and low amplitude. The input signal is furthermore delayed, cross multiplied and integrated to obtain a measure of the auto-correlation function of the input signal $s(t)$. Below is given an overview of the applied processing steps that transforms the measure of the auto-correlation function to a spectrum in the frequency domain:

- Accurate quantization correction requires accurate knowledge of the threshold levels used at quantization. The quantization correction used is only valid if the absolute values of the the positive and negative threshold levels are equal. The Odin/SMR correlators provide monitor channels to check the assumption of equal absolute values of the positive and negative threshold levels. Only when this condition is fulfilled the data will be further processed, otherwise the data will be blanked (filled with zeros).

- The estimation of the true correlation ρ from the measured correlation coefficient r at lag τ is then achieved by performing a quantization correction using Kulkarni and Heiles approximation described in Olberg et al. (2003).

- A Hanning smoothing is applied, which results in that the obtained resolution of the spectra is $2\,\mathrm{MHz}$ although the channel spacing is $1\,\mathrm{MHz}$

- The Fourier transform of the auto correlation function gives the power spectral density, or a spectrum in the frequency domain.

Radiances

The radiance emitted by a blackbody per frequency unit is

$$B_\nu = \frac{2h\nu^3}{c^2} \frac{1}{\exp(\frac{h\nu}{kT}) - 1}, \tag{2.1}$$

where ν is frequency, h is Planck's constant, k is Boltzmann's constant, c is the speed of light, and T is the physical temperature of the blackbody. The Rayleigh–Jeans correspondence (valid when $h\nu/kT \ll 1$) reads

$$B_v = \frac{2\nu^2 kT}{c^2}. \tag{2.2}$$

The Odin/SMR radiometers are heterodyne systems which receive a power (P_ν) per unit frequency range (spectral power density),

$$P_\nu = \frac{c^2}{2\nu^2} B_\nu \tag{2.3}$$

where ν is frequency, h is Planck's constant, k is Boltzmann's constant, when viewing a blackbody source at temperature (T) that completely fills the antenna field of view. If the Rayleigh–Jeans approximation is valid, we then have that

$$P_\nu = kT. \tag{2.4}$$

For a theoretical receiver and channel of bandwidth $\Delta\nu$, with zero loss and gain and a unit frequency response, the received power is

$$P = kT\Delta\nu. \tag{2.5}$$

Brightness temperature (T_b) and antenna temperature (T_a) are two closely related quantities. They are both defined with respect to a matching blackbody temperature. However, they differ in that T_b corresponds to radiance while T_a must be seen as a measure on power. The brightness temperature is defined as the physical temperature a blackbody would have to generate the same radiance as the one of concern. That is, for a given radiance I, T_b is defined as

$$I = B_v(T_b), \tag{2.6}$$

and in the Rayleigh–Jeans approximation this gives

$$T_b = \frac{c^2 I}{2k v^2}. \tag{2.7}$$

Hence, the Rayleigh–Jeans temperature of a blackbody can be written as

$$T_b = \frac{h\nu}{k} \frac{1}{\exp(\frac{h\nu}{kT}) - 1}. \tag{2.8}$$

The antenna temperature is defined as the temperature of an ideal black body that would result in the same received power at the antenna aperture as in the actual case, which gives that (using Rayleigh–Jeans approximation)

$$T_a = \frac{P}{k\Delta\nu} \tag{2.9}$$

A radiometer detects radiant power but the measured power can be converted to an antenna or brightness temperature or a radiance, but it should be remembered that it is only power that can actually be measured.
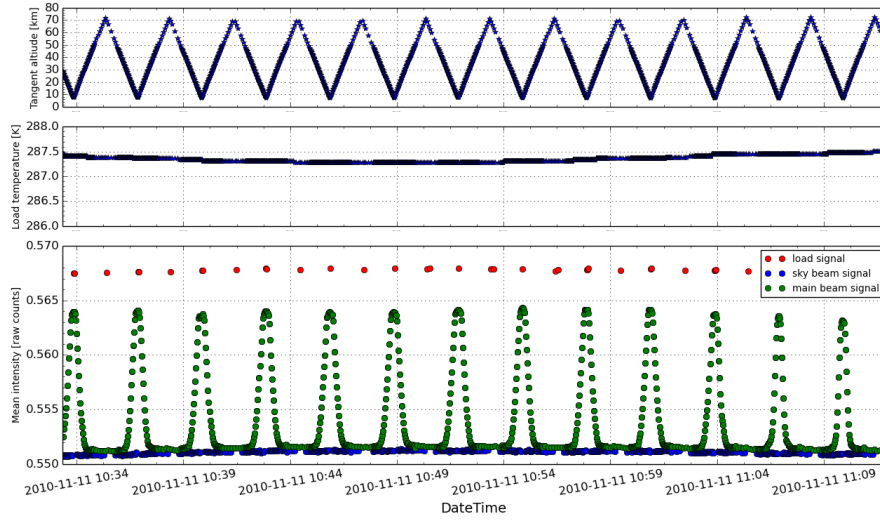
Figure 2.1: The upper panel shows the tangent altitude of the main beam for a number of scans. The middle panel shows the internal load temperature. The lower panel shows intensity variation, of one of the sub-bands of freqmode 1, for the three types of signals (described in text) involved in the intensity calibration scheme.

Odin/SMR observation sequence and measured signals

For calibration purposes, Odin/SMR performs areonomy observation in a switching mode, i.e. switching between the main beam and an unfocused sky beam. In nominal operation every other recorded signal comes from an unfocused cold sky beam, except around the lower and upper turning points of the scan where the reference beam is directed towards the internal load, typically three consecutive load spectra are recorded. The internal load acts as a blackbody emitter at an ambient temperature of around 285 K.

The intensity calibration of Odin/SMR is thus performed by using information from three types of signals (see Fig 2.1), i.e. the cold sky beam signal (c_s), the load signal (c_l), and the main beam signal (c_a). The calibration scheme is based on the assumption that the digital value (e.g. $c_{a,i}$) read out from channel i of the spectrometer is proportional to the power of the observed signal. The contributions to the three signals can be expressed as:

$$c_{a,i} = g_i \left(\eta_a T_{a,i} + T_{rec,i} + (1 - \eta_a) T_{amb,i} \right) = g_i \left(\eta_a T_{a,i} + T_{rec,i} + T_{sp} \right), \qquad (2.10)$$

$$c_{s,i} = g_i \left(T_{s,i} + T_{rec,i} \right) \approx g_i \left(T_{rec,i} \right), \qquad (2.11)$$

$$c_{l,i} = g_i \left(T_{l,i} + T_{rec,i} \right), \qquad (2.12)$$

where g_i is the receiver gain, η_a is the main beam efficiency (it is assumed that beam efficiencies for both the sky beam and load signals are unity), $T_{amb,i}$ is the receiver ambient temperature, and $T_{rec,i}$ is the receiver noise temperature. $T_{a,i}$, $T_{s,i}$, and $T_{l,i}$ are the antenna temperature, cosmic background temperature, and load temperature, all expressed as equivalent Rayleigh–Jeans brightness temperatures (T_b). The Rayleigh–Jeans brightness temperature of the cosmic background radiation at 500 GHz is only 0.003 K, (Eq. 2.8) and typical T_{rec} value of Odin/SMR is 3000 K, thus the approximation in eq. 2.11 results in negligible error.

The main beam signal is always at a higher level than the cold sky signal (Fig. 2.1), which is due to thermal emission from a baffle which only affects the main beam signal. Thus, the main beam intercepts with the baffle and the spill over contribution (T_{sp}):

$$T_{sp} = (1 - \eta_a)T_{amb}. \tag{2.13}$$

Calibration: basic equations

The aim of the calibration process is to use information from the signals described in Sect. 2.2.3 in order to derive an estimate of the antenna temperature. Here we derive expressions for how the unknown $T_{rec,i}$, g_i, T_{sp}, n_a, and $T_{a,i}$ can be derived. In Sect. 2.2.6 the actual Odin/SMR calibration is described.

Eq. 2.11 gives that

$$T_{rec,i} = \frac{c_{s,i}}{g_i}, \tag{2.14}$$

and g_i can be obtained from the difference between $c_{l,i}$ and $c_{s,i}$, i.e.

$$g_i = \frac{c_{l,i} - c_{s,i}}{T_{l,i} - T_{s,i}}. \tag{2.15}$$

By combining Eq. 2.14 and 2.15 we obtain

$$T_{rec,i} = c_{s,i}\frac{T_{l,i} - T_{s,i}}{c_{l,i} - c_{s,i}}. \tag{2.16}$$

$T_{a,i}$ can be obtained from the difference between between $c_{a,i}$ and $c_{s,i}$, i.e.

$$\begin{aligned} T_{a,i} &= \frac{1}{\eta_a}\left(\frac{c_{a,i} - c_{s,i}}{g_i} - T_{sp}\right) \\ &= \frac{1}{\eta_a}\left((c_{a,i} - c_{s,i})\frac{T_{rec,i}}{c_{s,i}} - T_{sp}\right). \end{aligned} \tag{2.17}$$

For measurements at tangent altitude above the atmosphere, $T_{a,i} = 0$. Thus, we have that for these measurements to a very good approximation

$$T_{sp,i} = (c_{a,i} - c_{s,i})\frac{T_{rec,i}}{c_{s,i}}. \tag{2.18}$$

Combining Eq. 2.13 and 2.18 gives that

$$\eta_a = 1 - \frac{T_{sp}}{T_{amb}} = 1 - \frac{(c_{a,i} - c_{s,i})\frac{T_{rec,i}}{c_{s,i}}}{T_{amb}}. \tag{2.19}$$

Ripple

Equation 2.17 can be thought of as the main intensity calibration equation for the Odin/SMR calibration scheme. In the derivation of Eq. 2.17 the reference signals are assumed to be "clean". In practice, there seems to be a small imbalance between measurements and references for Odin/SMR. Small perturbations of the sky and load signals will result in undesired features in calibrated spectra (which we denote as "ripple") if not taken into account (see Fig. 2.2). The sensitivity of calibrated $T_{a,i}$ to small perturbations on $T_{s,i}$ and $T_{l,i}$ are:

$$\frac{dT_{a,i}}{dT_{s,i}} = \frac{1}{\eta_a}\left(1 - \frac{c_{a,i} - c_{s,i}}{c_{l,i} - c_{s,i}}\right) \approx \frac{1}{\eta_a}\left(1 - \frac{T_{a,i}}{T_{l,i}}\right) \tag{2.20}$$

and

$$\frac{dT_{a,i}}{dT_{l,i}} = \frac{1}{\eta_a}\left(\frac{c_{a,i} - c_{s,i}}{c_{l,i} - c_{s,i}}\right) \approx \frac{1}{\eta_a}\left(\frac{T_{a,i}}{T_{l,i}}\right). \tag{2.21}$$

Thus, the sensitivity is linearly proportional to $T_{a,i}$. When $T_{a,i}$ is close to or 0 K (as it is for measurements at high tangent altitudes) the sensitivity to perturbations of the sky beam signal is at its maximum. On the other hand, perturbations on the load signal then have practically no impact on $T_{a,i}$. If $T_{a,i}$ were equal to the load temperature the situation would be reversed, though this is never the case in practice.

A model for the removal of the effects of ripple on the reference signals on estimated $T_{a,i}$ (from Eq. 2.17) to achieve a new better estimate $T'_{a,i}$ of the antenna temperature then reads

$$T'_{a,i} = T_{a,i} - \frac{1}{\eta_a}\left(1 - \frac{T_{a,i}}{T_{l,i}}\right)s_{0,i} - \frac{1}{\eta_a}\left(\frac{T_{a,i}}{T_{l,i}}\right)s_{1,i}, \tag{2.22}$$

where $s_{0,i}$ and $s_{1,i}$ can be seen as spectra that contain the ripple induced features for $T_{a,i}=0\,\text{K}$ and $T_{a,i}=load\ temperature$ respectively.

Intensity calibration scheme

The intensity calibration scheme can be divided into two parts. The first part can be seen as a scan based calibration scheme, in which the Equations of Sect. 2.2.4 are applied. The second part takes ripples (2.2.5) into account and uses the results (for a long period of time of measurements) from the first part of the calibration.

Part 1

The Odin calibration scheme (version 8) is scan-based, as will be described below, and this is one of the main differences to previous verisons.

Equation 2.17 is the key equation of the calibration. From this equation we see that to calibrate a given target signal we need to determine $T_{rec,i}$, T_{sp}, η_a, and $c_{s,i}$. The variables $T_{rec,i}$, T_{sp}, and η_a are assumed to be fairly stable over short time scales. Common values of all these parameters are used for the calibration of all c_a signals within a given scan. g can vary significant over short time-scales, and this is taken into account by the division of c_a with c_s (with a unique c_s for each c_a signal of the scan). The intensity calibration scheme (version 8) for a given scan can be summarized as:

- collect all relevant level0 and level1 data for the scan and for an additional time-period of ± 45 minutes. It is assured that only data with ssb attenuator settings as in the first load signal of the scan is used. Furthermore, only data where calibrated sky frequencies changes by less than 1 MHz from one signal to another is used.

- filter data, i.e. remove untrusted reference signals:
  Only sky beam signals from Sky Beam 1 (SK1) are used. An SK1 signal is only used if the previous reference signal was from SK1. SK1 signals with skybeamhit flags EARTH1, MOON1, and SUN1 are not used. Only the second load signal is used for each sequence of load signals observation.

- estimate an average T_{rec} spectrum:
  Equation 2.16 is applied to calculate T_{rec} for all kept c_l signals, where the two nearest c_s signals are linearly interpolated in time to c_l. The mean value of all T_{rec} is used as the common T_{rec} spectrum within a given scan.
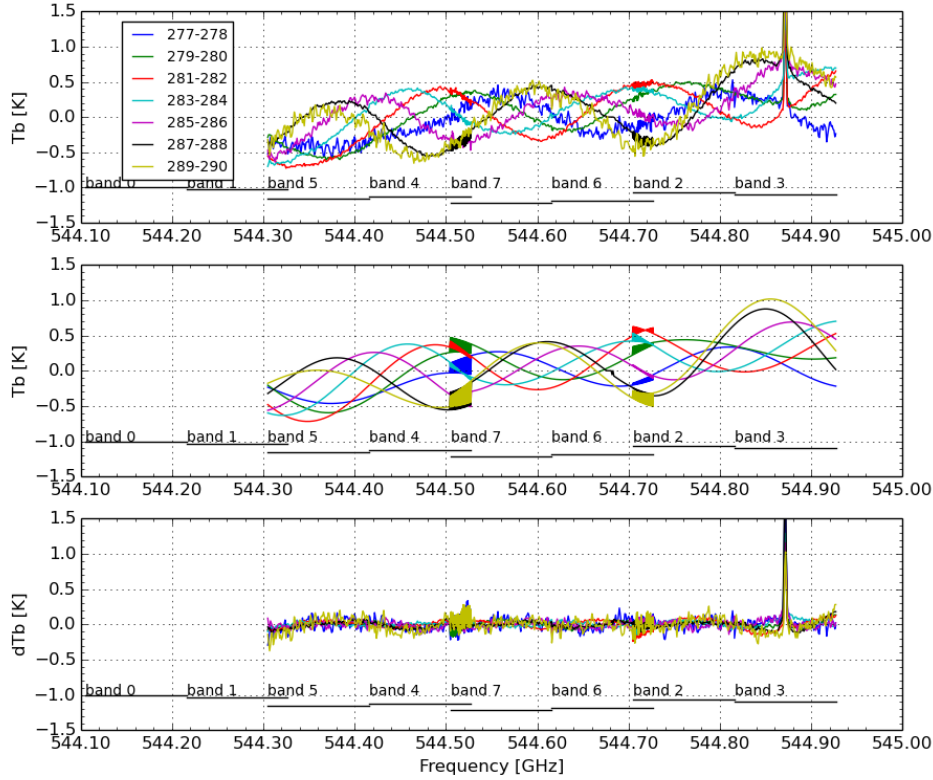
Figure 2.2: Schematic of part 2 of the intensity calibration. The upper panel shows uncorrected average spectra for frequency mode 2 observations with tangent points between 80 and 120 km. The color-coding corresponds to ambient temperature of the satellite (hot-load temperature). The middle panel shows fits of the ripple of the spectra in the upper panel. The lower panel shows the residual.

- estimation of a scalar T_{sp}:
  T_{sp} is estimated from measurements at high tangent altitude by applying Eq. 2.18. The median of the median from all c_a signals, measured within the top 10 km of the range of tangent altitudes, is used as a common scalar T_{sp}.

- estimation of η_a:
  η_a is estimated by applying Eq. 2.19, using the estimated T_{sp} described above, and an assumed T_{amb} of 300 K.

- estimate T_a:
  apply Eq. 2.17, using the estimated parameters as described above and the two nearest c_s signals are linearly interpolated in time to c_a.

Part 2

Part 2 of the calibration deals with the removal of the effects of ripple on the sky signal on calibrated spectra from part 1, which neglects this effect. The removal of the artifacts introduced by the sky signal ripple is a fairly straight-forward task, as the artifacts can

be estimated from high tangent point measurements where we know that the intensity of a calibrated spectrum should be 0 K.

Ripple on the load signal is more complicated from a calibration perspective. The artifacts, in calibrated atmospheric spectra, from ripple on the load signal can be seen as weak signal on top of a strong atmospheric signal, and thus not easy to detect. For this reason, we leave this effect unresolved.

Figure 2.2 shows median spectra of calibrated (Part 1) spectra from measurements at high tangent altitudes for one of the observation mode of AC1 (for the further discussion on this figure ignore the left-most part of the spectra, which comes from two problematic bands of AC1 that should not be used). These spectra are expected to be centered around 0 K (except for the ozone line between 544.8–544.9 GHz), but due to ripple in the sky signal we can see a wave pattern in the spectra. Figure 2.2 also indicates that the phase of the wave pattern depends on the measurement conditions, and the temperature of the load (ambient temperature) is used in Fig 2.2 to describe the measurement condition.

The calibration scheme (Part 2) is as follows:

- Extract median spectra of calibrated spectra (from Part 1:ac_level1b table) from measurements at tangent altitudes above 80 km for a range of hot load temperatures ([277–278 K, 278–279 K, ..., 289–290 K]) for each observation mode, and import the spectra into the ac_level1b_average table

- Estimate a fit to the median spectrum for each mode by

  1. applying a filter that removes channels which are contaminated by atmospheric information or lines from the median spectrum
  2. using the target fitting function

  $$y = a + b\sin(cf + d) \tag{2.23}$$

  where f is the frequency and a, b, c, d parameters to estimate, in order to fit the spectrum for each of the four modules of AC1 or AC2. The fitting is performed in such a way that c is forced to be equal for all of the four modules. Import the fit into the ac_cal_level1c table

- Apply the correction.
  Equation 2.22 is applied to correct a given calibrated spectrum (from part 1), where the fit of the median spectrum with matching hot load temperature range is used as the s_0 spectrum.

Radiometric performance and uncertainties

In this section we deal with uncertainties that are related to calibrated Odin/SMR spectra. In Sect. 2.3.1 we describe uncertainties related to radiometric noise. In Sect. 2.3.2 we describe uncertainties related to rapid gain fluctuations. In Sect. 2.3.3 we describe uncertatinties that are related to imperfect knowledge of load temperature and main beam efficiency. In Sect. 2.3.4 trend uncertainties are explored. In Sect. 2.3.5 we describe the noise correlations. In Sect. 2.3.6 we describe the noise estimate output from the calibration routine.

Table 2.1: Average T_{rec}, T_{sp}, and radiometric noise (for 1.8 sec. integration time) for the various frequency modes

Backend	Frontend	LO freq [GHz]	FM	T_{rec} [K]	T_{sp} [K]	$\Delta T[K]$
AC1	495 A2	492.750	23	3000	7.0	2.0
		499.698	25	3500 *	6.2	-
	549 A1	548.502	2	2800 *	8.0	1.8
		553.050	19	2900 *	7.3	1.9
		547.752	21	3100 *	8.6	2.0
		553.302	23	3200	6.8	2.1
	555 B2	553.298	13	3200	14.0	2.1
	572 B1	572.762	24	3200 *	9.4	2.1
AC2	495 A2	497.880	1	3200	6.1	2.1
		492.750	8	3200	7.4	2.1
		494.750	17	3200	6.7	2.1
		499.698	25	3200	7.6	2.1
	572 B1	572.762	14	3700 *	9.9	2.4
		572.964	22	3700 *	10.0	2.4

Uncertainties related to radiometric noise

In the Odin/SMR calibration process three types of signals are used (all of them containing radiometric noise) and the obtained noise in calibrated spectra is sensitive to noise in all of these measurements. The noise contribution can be divided into three terms (1) the radiometer noise contribution, (2) interpolated reference noise contribution, and (3) interpolated gain noise contribution Jarnot et al. (2004).

These contributions (derived in the following sub-sections) gives that the noise on an individual channel ΔT_i of a calibrated Odin/SMR spectrum using the calibration scheme described in Sect. 2.2.6. The noise can be described by

$$\Delta T_i^2 = \frac{1}{B\tau} \left((T_{rec,i} + T_{a,i})^2 + \frac{T_{rec,i}^2}{2} + \frac{T_{a,i}^2}{n} \left(\left(\frac{T_{rec,i} + T_{l,i}}{T_{l,i}} \right)^2 + \left(\frac{T_{rec,i}}{T_{l,i}} \right)^2 \right) \right). \quad (2.24)$$

For measurements with a nearly blank background (i.e. $T_{a,i} \approx 0$), uncertainties in the gain estimate have low impact and the noise expression reduces to

$$\Delta T_i = T_{rec,i} \sqrt{\frac{3}{2} \frac{1}{B\tau}}. \quad (2.25)$$

In Table 2.1 typical T_{rec} values and radiometric noise levels (for measurements having high tangent points) of the main frequency modes of Odin/SMR are listed.

As a starting point to derive Eq. 2.24 we take the derivative of $T_{a,i}$ with respect to $c_{a,i}$, $c_{s,i}$, and g_i:

$$\frac{\partial T_{a,i}}{\partial c_{a,i}} \approx \frac{1}{g_i}, \quad (2.26)$$

$$\frac{\partial T_{a,i}}{\partial c_{s,i}} \approx \frac{1}{g_i}, \quad (2.27)$$

$$\frac{\partial T_{a,i}}{\partial g_i} \approx -\frac{c_{a,i} - c_{s,i}}{g_i^2} \approx \frac{T_{a,i}}{g_i}, \quad (2.28)$$

which implies:

$$\Delta T_i^2 = \frac{\Delta c_{a,i}^2}{g_i^2} + \frac{\Delta c_{s,i}^2}{g_i^2} + T_{a,i}^2 \frac{\Delta g_i^2}{g_i^2}, \tag{2.29}$$

where the terms on the right hand side is (1) the radiometer noise contribution, (2) interpolated reference noise contribution, and (3) interpolated gain noise contribution. In the following sections these terms are described in more detail.

Precision: radiometer noise contribution

The radiometer noise contribution induced noise variance in calibrated $T_{a,i}$ is simply

$$\frac{\Delta c_{a,i}^2}{g_i^2} = \frac{T_{sys}^2}{B\tau}. \tag{2.30}$$

Precision: interpolated reference noise contribution

In the Odin/SMR calibration scheme, and for the nominal situation, the sky beam interpolated reference signal can be written

$$\hat{c}_{s,i}(t_{j+1}) = \frac{1}{2} c_{s,i}(t_j) + \frac{1}{2} c_{s,i}(t_{j+2}), \tag{2.31}$$

where t_j represent time. If the gain fluctuations are small or follow a linear variation during the observation sequence, the noise in $\hat{c}_{s,i}(t_{j+1})$ is only due to radiometric noise and induced noise variance in calibrated $T_{a,i}$ is

$$\frac{\Delta c_{s,i}^2}{g_i^2} = \frac{T_{rec}^2}{2B\tau}. \tag{2.32}$$

In practice there is also a finite error due to non-linear and non-captured gain variation and this is described in Sect 2.3.2.

Precision: interpolated gain noise contribution

In the calibration scheme, the gain is estimated as

$$g_i(t_{j+k}) = \frac{\hat{c}_{s,i}(t_{j+k})}{\overline{T}_{rec,i}} = \hat{c}_{s,i}(t_{j+k}) \left(\frac{1}{n} \sum_{j=1}^{n} T_{rec,i}(t_j) \right)^{-1}, \tag{2.33}$$

where

$$T_{rec,i}(t_j) = \hat{c}_{s,i}(t_j) \frac{T_l - T_s}{c_{l,i}(t_j) - \hat{c}_{s,i}(t_j)}. \tag{2.34}$$

That is, the precision of the interpolated gain depends on the precision of an interpolated reference measurement and on an average T_{rec}.

We first note that

$$\frac{\partial g_i}{\partial \hat{c}_{s,i}(t_{j+k})} = \frac{1}{\overline{T}_{rec,i}} \tag{2.35}$$

$$\frac{\partial g_i}{\partial T_{rec,i}} = -\frac{\hat{c}_{s,i}(t_{j+k})}{\overline{T}_{rec,i}^2}. \tag{2.36}$$

For an individual T_{rec} estimate, we have that

$$\frac{\partial T_{rec,i}}{\partial c_{s,i}(t_j)} = \frac{(T_l - T_s)(c_{l,i} - c_{s,i}) + c_{s,i}(T_l - T_s)}{(c_{l,i} - c_{s,i})^2} \approx \frac{T_{rec,i}}{g_i T_l} \tag{2.37}$$

$$\frac{\partial T_{rec,i}}{\partial c_{l,i}} = \frac{-c_{s,i}(T_l - T_s)}{(c_{l,i} - c_{s,i})^2} \approx -\frac{T_{rec,i}}{g_i T_l} \tag{2.38}$$

Thus, we have

$$\frac{\partial g_i}{\partial c_{l,i}} = \frac{\partial g_i}{\partial T_{rec,i}} \frac{\partial T_{rec_i}}{\partial c_{l,i}} = \frac{1}{T_{l,i} - T_{s,i}} \tag{2.39}$$

$$\frac{\partial g_i}{\partial c_{s,i}} = \frac{\partial g_i}{\partial T_{rec,i}} \frac{\partial T_{rec_i}}{\partial c_{s,i}} = \frac{-1}{T_{l,i} - T_{s,i}} \tag{2.40}$$

which implies:

$$\Delta g_i^2 = \frac{\Delta c_{l,i}^2 + \Delta c_{s,i}^2}{(T_{l,i} - T_{s,i})^2} + \frac{\Delta c_i^2(t_{j+1})}{T_{rec,i}^2} \approx \frac{\Delta c_{l,i}^2 + \Delta c_{s,i}^2}{T_{l,i}^2} \tag{2.41}$$

and

$$T_{a,i}^2 \frac{\Delta g_i^2}{g_i^2} = \frac{T_{a,i}^2}{T_{l,i}^2} \frac{\Delta c_{l,i}^2 + \Delta c_{s,i}^2}{g_i^2}, \tag{2.42}$$

or, if we take into account that T_{rec} spectrum is an average from n measurements

$$T_{a,i}^2 \frac{\Delta g_i^2}{g_i^2} = \frac{1}{B\tau} \left(\frac{T_{a,i}^2}{n} \left(\left(\frac{T_{rec,i} + T_{l,i}}{T_{l,i}} \right)^2 + \left(\frac{T_{rec,i}}{T_{l,i}} \right)^2 \right) \right). \tag{2.43}$$

Uncertainties related to rapid gain fluctuations

In the preceding section we derived an error for reference noise contribution. Gain fluctuations on a small time scale (between reference-target-reference observation sequence) not captured by the interpolation of reference signals give rise to errors. In practice there is also a finite error due to non-linear gain variation i.e. there is a broadband-offset between the estimated and true reference signal

$$\hat{c}_s(t_{j+1}) - c_s(t_{j+1}) = \Delta c_s = \Delta g' T_{rec}, \tag{2.44}$$

where $\Delta g'$ represents the non-captured variation in gain due to non-linear gain fluctuations.

This error can be described as

$$\Delta T_{i,gain}^2 = T_{rec}^2 \left(\frac{\Delta g'}{g} \right)^2. \tag{2.45}$$

For a given Odin/SMR spectrum $\Delta T_i \approx 2\,\text{K}$ due to this effect, but when averaging many spectra this effect goes to 0.

Other uncertainties

There are also errors in calibrated Odin/SMR spectra due to imperfect knowledge of the calibration target temperature and main beam efficiency.

- The accuracy of temperature information of the calibration target is (ΔT_l) around 0.2 K. The related calibration error (ΔT_a) is

$$\Delta T_a \approx \frac{T_a}{T_l}\Delta T_l, \tag{2.46}$$

which gives that for observations against a blank background the error is close to 0, while if T_a=200 K $\Delta T_a \approx$ 0.14 K.

- Main beam efficiency uncertainty. The main beam efficiency is estimated for each scan and this estimate introduces a finite error to calibrated spectrum. We have that

$$\Delta T_a = \frac{\Delta n_a}{n_a}T_a, \tag{2.47}$$

and

$$\Delta n_a^2 = \left(\frac{T_{sp}\Delta T_{amb}}{T_{amb}^2}\right)^2 + \left(\frac{\Delta T_{sp}}{T_{amb}}\right)^2. \tag{2.48}$$

Thus, error in estimated main beam effciency is sensitive to errors in both assumed T_{amb} and estimated T_{sp}, and

$$\Delta T_a = \sqrt{\left(\frac{T_{sp}\Delta T_{amb}}{T_{amb}^2}\right)^2 + \left(\frac{\Delta T_{sp}}{T_{amb}}\right)^2}\frac{T_a}{n_a} \tag{2.49}$$

For the moment we assume that ΔT_{sp}=0 (see Sect. 2.3.4 for further analysis), and focus on the ΔT_{amb} term. There is no temperature sensor on Odin/SMR that measure the baffle temperature, and a constant value of 300 K is used in calibration process. Anyhow, for observations against a blank backgrund the error is close to 0, while if T_a=200 K, T_{amb}=300 K, T_{sp}=8 K, and ΔT_{amb}=10 K, than $\Delta T_a \approx$ 0.18 K.

Trend uncertainties

It can not be ruled out that calibrated Odin/SMR spectra contain artificial trends that are related to a possible error in the estimation of main beam efficiency.

The main beam efficiency is determined based on an estimated T_{sp} value (see Eq. 2.19). The estimation of T_{sp} (see Eq. 2.18) is done under the assumption that reference signals are "clean". It has been noted that there is a slight mismatch between main beam and reference signals (see Sect. 2.2.5). If we assume that the reference signal contains a time varying broadband offset $(c_s = g(T_{rec} + \Delta T_{off}(t)))$ we have that Eq. 2.18 reads

$$T_{sp} = (c_a - c_s)\frac{T_{rec}}{c_s} \approx (1 - \eta_a)T_{amb} - \Delta T_{off}(t), \tag{2.50}$$

thus, T_{sp} is made up of two contributions and the error in "true" T_{sp} is $\Delta T_{off}(t)$. Equation 2.49 then tells us how this related error introduces an error in estimated T_a within the calibration algorithm. Since main beam efficiency error is proportional to T_a it has low impact on weak signals. However, if $\Delta T_{off}(t)$ has changed by 1.5 K during the mission, one would see an artificial change in strong signals (around 200 K) of about 1 K.

Notes on noise correlations

Noise on calibrated Odin/SMR has correlations of the following type/reason:

- Radiometric noise from the target signal is correlated between neighboring channels of a given spectrum (due to Hanning smoothing).

- The gain variation term (Eq. 2.45) has been found to be correlated between channels for Odin/SMR̈This gain variation has been estimated to give rise to a constant shift in the brightness temperature across the band (that is, it can be seen as a flat baseline ripple), where the shift has a standard deviation of about 2 K and is uncorrelated between tangent altitudes and front-ends.

  > Add reference or show figure

- Noise of two neighboring spectra is correlated due to the fact that they share (1) cold sky reference measurements. The noise linear correlation coefficient from a given channel from two neighboring spectra should be ~ 0.17 due to this fact. This value was derived from simulations for an ideal case, in which simulated measurements and references were given noise of equal magnitude, and the calibration process replicated.

- All spectra in a scan share a common (noisy) T_{rec} spectrum.

Precision: estimates from calibration process

T_{rec} and obtained random uncorrelated noise level is estimated within the calibration processing for each scan.

This random noise level is estimated as an effective integration time (τ_{eff}) from calibrated spectra of the upper part of a scan (with a blank background). Each spectrum of a scan is given an effective integration time, but it is determined from all spectra within a time window of ± 45 minutes. Within the calibration algorithm, the noise of each sub-band of the considered spectrum is calculated as the bias corrected variance, i.e.

$$\Delta T^2 = \frac{1}{n-1} \sum_{i=1}^{n} (T_{b,i} - \langle T_b \rangle)^2 \tag{2.51}$$

An efficiency factor η for each sub-band is then calculated (from the radiometer noise equation) as

$$\eta = \frac{T_{rec}^2}{B \Delta T^2 \tau}. \tag{2.52}$$

An efficiency factor for the scan is then determined from the sub-band with the highest average efficiency factor. The alternative option to use the result from the sub-band with lowest efficiency factor is not wise. The reason is that even for spectra of the upper part of the scan, some sub-bands may contain the signature of an emission line which would be treated as noise here.

The effective integration time associated with a given spectrum in the Level1B data should then be treated as a variable that can be plugged into the radiometer noise equation, i.e.

$$\Delta T = T_{rec} \frac{1}{\sqrt{B \tau_{eff}}}, \tag{2.53}$$

to obtain a measure of the noise level of the spectrum (and B should be set to 100 MHz although this is not the resolution of a channel after calibration). This obtained noise level should be comparable to the noise of Eq. 2.25.

Table 2.2: Fitting parameters for the frequency drift correction.

Frontend	Constant	Time Dependence	Temperature dependence
	c_0	c_0	c_0
555	1.00007687	$-9.881469 \cdot 10^{-10}$	$-7.20429255 \cdot 10^{-8}$
495	1.00004369	$-3.049353 \cdot 10^{-10}$	$-9.77071337 \cdot 10^{-8}$
549	1.00005847	$-6.275934^* \cdot 10^{-10}$	$-3.89089138 \cdot 10^{-8}$
572	N/A	N/A	N/A

Frequency calibration

Local oscillator frequency drift

Firstly, the operating local oscillator (LO) frequency is calculated from harmonic reference oscillator and phase locked loop (PLL) reference oscillator frequencies from the housekeeping level0 data. A second step is then to account for drifts in the LO frequency. It has been previously noted that a spectral shift exists in the current level 1 dataset (version 6 and 7) and that this shift has been changing over time. A new model, based on Version 2-0 and Verison 2-1 Level2 data, is applied for calibration version 8 data that takes into account of a temperature dependency and a temporal term of the LO frequency drift. The correction factor k and frequency drift corrected LO frequency $\hat{f}_{lo,sky}$ is estimated as

$$k = c_0 + c_1 \cdot mjd + c_2 \cdot T_{pll} \tag{2.54}$$

and

$$\hat{f}_{lo,sky} = k f_{lo,sky}, \tag{2.55}$$

where T_{pll} is the temperature of image load b-side, and the c_0, c_1, and c_2 terms have been found to depend on the applied frontend and the applied values are displayed in Table 2.2. Another correction is applied for data from the 572 GHz frontend. Due to a PLL failure of this radiometer, which in practice means that the LO frequency is noticeably offset from the commanded frequency, a special correction is applied in the Level1 processing, which is described in Appendix D. This model keeps the frequency error within ± 0.5 MHz (except for data from the 572 GHz radiometer).

Doppler correction

A Doppler correction is applied. The relative velocity v_{geo} of the satellite in the direction of the tangent point is used to translate the LO frequency to an earth-fixed reference frame. i.e.

$$\hat{f}_{lo} = \hat{f}_{lo,sky}/(1.0 - v_{geo}/c), \tag{2.56}$$

where c is the speed of light.

Pointing and attitude data processing

The vertical scanning is achieved by rotation of the satellite platform by an advanced attitude control system (ACS). The ACS uses star trackers as the main sensors with backup from gyros, magnetometers, and Sun sensors. Reaction wheels and magnetic coils serve as actuators. The ACS pointing accuracy in limb-scanning mode is $5'$ in real time

knowledge, and better than $1'$ in reconstructed knowledge (which translates to a $\sim 800\,\text{m}$ accuracy in tangent point).

The reconstructed attitude data files contain the estimated achieved attitude given as a quaternion, and the satellite position and velocity from GPS receiver on-board of Odin.

In the calibration software at Chalmers, this data is used to calculate the geographical position of the tangent point, the satellite relative velocity v_{geo} of the satellite in the direction of the tangent point. The hit of the target and sky beams with various objects (e.g. Earth, Moon) are also tested (using a low precision ephemeris) and reported as quality indicators.

Level1B data format and quality

Data format

Odin/SMR Level0 and Level1B data are stored in tables in a calibration database at the Dept. of Earth and Space Sciences at Chalmers University of Technology (Chalmers) in Gothenburg. There are several ways to access the data but the recommendation is to access data through the Odin/SMR web-page http://malachite.rss.chalmers.se. On the Odin/SMR web-page Level1b and auxiliary data are basically displayed in three different views (frequency mode view, scan info view, and scan data view) with different levels of information details, as explained below:

1. Frequency mode view: displays which frequency modes that were deployed for a given date in Json format. For exmple, the URL http://malachite.rss.chalmers.se/rest_api/v4/freqmode_info/2015-01-03/ displays this information for 2015-01-03 and the content is given as:

```
{
  "Date": "2015-01-03",
  "Info": [
    {
      "Backend": "AC1",
      "FreqMode": 2,
      "NumScan": 481,
      "URL": "http://malachite.rss.chalmers.se/rest_api/v4/freqmode_info/2015-01-03/AC1/2"
    },
    {
      "Backend": "AC1",
      "FreqMode": 21,
      "NumScan": 241,
      "URL": "http://malachite.rss.chalmers.se/rest_api/v4/freqmode_info/2015-01-03/AC1/21"
    },
    {
      "Backend": "AC2",
      "FreqMode": 1,
      "NumScan": 481,
      "URL": "http://malachite.rss.chalmers.se/rest_api/v4/freqmode_info/2015-01-03/AC2/1"
    },
    {
      "Backend": "AC2",
      "FreqMode": 8,
      "NumScan": 125,
      "URL": "http://malachite.rss.chalmers.se/rest_api/v4/freqmode_info/2015-01-03/AC2/8"
    },
    {
      "Backend": "AC2",
      "FreqMode": 17,
      "NumScan": 122,
      "URL": "http://malachite.rss.chalmers.se/rest_api/v4/freqmode_info/2015-01-03/AC2/17"
    }
  ]
}
```

For this date it can be seen that five different frequency modes (FreqMode) were deployed. For each frequency mode an URL is given where more detailed information of the scans (NumScan=number of scans) from this date can be obtained, as explained below.

2. scan info view: displays log data in Json format for each scan from a given date and frequency mode. As example, the URL http://malachite.rss.chalmers.se/rest_api/v4/freqmode_info/2015-01-03/AC1/2/ displays scan info data for all frequency mode 2 scans from 2015-01-03, and the data for the first scan is shown below (the fields are described in Table 3.1):

```
{
  "Info": [
    {
      "AltEnd": 3450.29,
      "AltStart": 66787.300000000003,
      "DateTime": "2015-01-03T11:42:32.184000",
      "FreqMode": 2,
      "LatEnd": -6.4216600000000001,
      "LatStart": -13.2338,
      "LonEnd": 100.09699999999999,
      "LonStart": 100.711,
      "MJDEnd": 57025.488372699998,
      "MJDStart": 57025.487372299998,
      "NumSpec": 33,
      "ScanID": 7003000326,
      "SunZD": 90.695250000000001,
      "URLS": {
        "URL-apriori-BrO": "http://malachite.rss.chalmers.se/rest_api/v4/apriori/BrO/2015-01-03/AC1/2/7003000326",
        "URL-apriori-C2H2": "http://malachite.rss.chalmers.se/rest_api/v4/apriori/C2H2/2015-01-03/AC1/2/7003000326",
        "URL-apriori-C2H6": "http://malachite.rss.chalmers.se/rest_api/v4/apriori/C2H6/2015-01-03/AC1/2/7003000326",
        "URL-apriori-CH3CN": "http://malachite.rss.chalmers.se/rest_api/v4/apriori/CH3CN/2015-01-03/AC1/2/7003000326",
        "URL-apriori-CH3Cl": "http://malachite.rss.chalmers.se/rest_api/v4/apriori/CH3Cl/2015-01-03/AC1/2/7003000326",
        "URL-apriori-CH4": "http://malachite.rss.chalmers.se/rest_api/v4/apriori/CH4/2015-01-03/AC1/2/7003000326",
        "URL-apriori-CO": "http://malachite.rss.chalmers.se/rest_api/v4/apriori/CO/2015-01-03/AC1/2/7003000326",
        "URL-apriori-CO2": "http://malachite.rss.chalmers.se/rest_api/v4/apriori/CO2/2015-01-03/AC1/2/7003000326",
        "URL-apriori-COF2": "http://malachite.rss.chalmers.se/rest_api/v4/apriori/COF2/2015-01-03/AC1/2/7003000326",
        "URL-apriori-Cl2O2": "http://malachite.rss.chalmers.se/rest_api/v4/apriori/Cl2O2/2015-01-03/AC1/2/7003000326",
        "URL-apriori-ClO": "http://malachite.rss.chalmers.se/rest_api/v4/apriori/ClO/2015-01-03/AC1/2/7003000326",
        "URL-apriori-ClONO2": "http://malachite.rss.chalmers.se/rest_api/v4/apriori/ClONO2/2015-01-03/AC1/2/7003000326",
        "URL-apriori-ClOOCl": "http://malachite.rss.chalmers.se/rest_api/v4/apriori/ClOOCl/2015-01-03/AC1/2/7003000326",
        "URL-apriori-H2CO": "http://malachite.rss.chalmers.se/rest_api/v4/apriori/H2CO/2015-01-03/AC1/2/7003000326",
        "URL-apriori-H2O": "http://malachite.rss.chalmers.se/rest_api/v4/apriori/H2O/2015-01-03/AC1/2/7003000326",
        "URL-apriori-H2O2": "http://malachite.rss.chalmers.se/rest_api/v4/apriori/H2O2/2015-01-03/AC1/2/7003000326",
        "URL-apriori-H2S": "http://malachite.rss.chalmers.se/rest_api/v4/apriori/H2S/2015-01-03/AC1/2/7003000326",
        "URL-apriori-HBr": "http://malachite.rss.chalmers.se/rest_api/v4/apriori/HBr/2015-01-03/AC1/2/7003000326",
        "URL-apriori-HCN": "http://malachite.rss.chalmers.se/rest_api/v4/apriori/HCN/2015-01-03/AC1/2/7003000326",
        "URL-apriori-HCOOH": "http://malachite.rss.chalmers.se/rest_api/v4/apriori/HCOOH/2015-01-03/AC1/2/7003000326",
        "URL-apriori-HCl": "http://malachite.rss.chalmers.se/rest_api/v4/apriori/HCl/2015-01-03/AC1/2/7003000326",
        "URL-apriori-HF": "http://malachite.rss.chalmers.se/rest_api/v4/apriori/HF/2015-01-03/AC1/2/7003000326",
        "URL-apriori-HI": "http://malachite.rss.chalmers.se/rest_api/v4/apriori/HI/2015-01-03/AC1/2/7003000326",
        "URL-apriori-HNO3": "http://malachite.rss.chalmers.se/rest_api/v4/apriori/HNO3/2015-01-03/AC1/2/7003000326",
        "URL-apriori-HO2": "http://malachite.rss.chalmers.se/rest_api/v4/apriori/HO2/2015-01-03/AC1/2/7003000326",
        "URL-apriori-HOBr": "http://malachite.rss.chalmers.se/rest_api/v4/apriori/HOBr/2015-01-03/AC1/2/7003000326",
        "URL-apriori-HOCl": "http://malachite.rss.chalmers.se/rest_api/v4/apriori/HOCl/2015-01-03/AC1/2/7003000326",
        "URL-apriori-N2": "http://malachite.rss.chalmers.se/rest_api/v4/apriori/N2/2015-01-03/AC1/2/7003000326",
        "URL-apriori-N2O": "http://malachite.rss.chalmers.se/rest_api/v4/apriori/N2O/2015-01-03/AC1/2/7003000326",
        "URL-apriori-NH3": "http://malachite.rss.chalmers.se/rest_api/v4/apriori/NH3/2015-01-03/AC1/2/7003000326",
        "URL-apriori-NO": "http://malachite.rss.chalmers.se/rest_api/v4/apriori/NO/2015-01-03/AC1/2/7003000326",
        "URL-apriori-NO2": "http://malachite.rss.chalmers.se/rest_api/v4/apriori/NO2/2015-01-03/AC1/2/7003000326",
        "URL-apriori-O2": "http://malachite.rss.chalmers.se/rest_api/v4/apriori/O2/2015-01-03/AC1/2/7003000326",
        "URL-apriori-O3": "http://malachite.rss.chalmers.se/rest_api/v4/apriori/O3/2015-01-03/AC1/2/7003000326",
        "URL-apriori-OBrO": "http://malachite.rss.chalmers.se/rest_api/v4/apriori/OBrO/2015-01-03/AC1/2/7003000326",
        "URL-apriori-OCS": "http://malachite.rss.chalmers.se/rest_api/v4/apriori/OCS/2015-01-03/AC1/2/7003000326",
        "URL-apriori-OClO": "http://malachite.rss.chalmers.se/rest_api/v4/apriori/OClO/2015-01-03/AC1/2/7003000326",
        "URL-apriori-OH": "http://malachite.rss.chalmers.se/rest_api/v4/apriori/OH/2015-01-03/AC1/2/7003000326",
        "URL-apriori-SF6": "http://malachite.rss.chalmers.se/rest_api/v4/apriori/SF6/2015-01-03/AC1/2/7003000326",
        "URL-apriori-SO2": "http://malachite.rss.chalmers.se/rest_api/v4/apriori/SO2/2015-01-03/AC1/2/7003000326",
        "URL-ptz": "http://malachite.rss.chalmers.se/rest_api/v4/ptz/2015-01-03/AC1/2/7003000326",
        "URL-spectra": "http://malachite.rss.chalmers.se/rest_api/v4/scan/AC1/2/7003000326"
      }
    },
.
.
. # in this example only data from one scan is displayed
.
}
```

As can be seen, the data structure contains a number of URLs. These URLs displays more detailed data (Level1B and auxiliary data) as described below.

3. scan data view: displays Level1B and auxiliary data in Json format for a scan. Three different views are available, and example URLS are give below:

- for Level1B `http://malachite.rss.chalmers.se/rest_api/v4/scan/AC1/2/7002887494/`, Table 3.2 gives a description of the data fields.

- for PTZ data (pressure,temperature, and altitude data) `http://malachite.rss.chalmers.se/rest_api/v4/ptz/2015-01-03/AC1/2/7002887494` Table 3.3 gives a description of the data fields.

- for *a priori* O_3 data `http://malachite.rss.chalmers.se/rest_api/v4/apriori/O3/2015-01-03/AC1/2/7002887494/`, (see the scan info view above for other available *a priori* data). Table 3.4 gives a description of the data fields.

Table 3.1: Odin scan log data format. Latitudes and longitudes are given as geodetic coordinates using WGS84 reference ellipsoid. Example URL http://malachite.rss.chalmers.se/rest_api/v4/freqmode_info/2015-01-03/AC1/2/

Variable	Description
AltEnd	*(Double)*: Tangent point altitude ([m]) for last spectrum in scan.
AltStart	*(Double)*: Tangent point altitude for first spectrum in scan.
DateTime	*(String)*: Mean UTC datetime (datetime(firts) + datetime(last))/2 of scan.
LatEnd	*(Double)*: Latitude of tangent point for last spectrum in scan.
LatStart	*(Double)*: Latitude at tangent point for first spectrum in scan.
LonEnd	*(Double)*: Longitude of tangent point for last spectrum in scan.
LonStart	*(Double)*: Longitude at tangent point for first spectrum in scan.
FreqMode	*(Integer)*: Deployed frequency mode.
MJDEnd	*(Double)*: Modified julian date for last spectrum in scan.
MJDStart	*(Double)*: Modified julian date for first spectrum in scan.
NumSpec	*(Integer)*: Number of atmospheric spectra in scan.
ScanID	*(Integer)*: Satellite time word identifier of scan.
SunZD	*(Double)*: Mean solar zenith angle (SunZD(first) + SunZD(last))/2 for scan.
URLS	URLs to more detailed information of scan. • URL-spectra: link to scan Leve1B-data (see Table 3.2) • URL-ptz: link to scan PTZ-data (see Table 3.3) • URL-apriori-*species* link to available scan apriori data (see Table 3.4), where *species* can be any of: 'BrO', 'Cl2O2', 'CO', 'HCl', 'HO2', 'NO2', 'OCS', 'C2H2', 'ClO', 'H2CO', 'HCN', 'HOBr', 'NO', 'OH', 'C2H6', 'ClONO2', 'H2O2', 'HCOOH', 'HOCl', 'O2', 'SF6', 'CH3Cl', 'ClOOCl', 'H2O', 'HF', 'N2', 'O3', 'SO2', 'CH3CN', 'CO2', 'H2S', 'HI', 'N2O', 'OBrO', 'CH4', 'COF2', 'HBr', 'HNO3', 'NH3', 'OClO'

Table 3.2: Odin/SMR scan data format. Example URL: http://malachite.rss.chalmers.se/rest_api/v4/scan/AC1/2/7003000326

Variable	Description
Version	*(Array of integers)*: Calibration version.
Quality	*(Array of integers)*: Quality indicator of scan/spectrum (see Table 3.5).
STW	*(Array of integers)*: Satellite time word.
MJD	*(Array of doubles)*: Modified julian date of observation.
Orbit	*(Array of doubles)*: Number of orbit plus fraction.
Spectrum	*(2-D Array of doubles)*: Frequency sorted and intensity calibrated spectra in Rayleigh Jeans temperature in Kelvin.
TrecSpectrum	*(Array of doubles)*: Frequency sorted receiver noise temperature spectrum determined and used in calibration of this scan.
Frontend	*(Array of integers)*: The frontend used for this observation: $1 = 555$, $2 = 495$, $3 = 572$, $4 = 549$, and $5 = 119$.
Backend	*(Array of integers)*: The backend used for this observation: $1 = $ AC1 and $2 = $ AC2
RA2000	*(Array of doubles)*: The right ascension (J2000) of the direction of pointing in degrees.
Dec2000	*(Array of doubles)*: The declination (J2000) of the direction of pointing in degrees.
Longitude	*(Array of doubles)*: Geodetic latitude of the tangent point.
Latitude	*(Array of doubles)*: Geodetic latitude of the tangent point.
Altitude	*(Array of doubles)*: Tangent point altitude [m].
GPSpos	*(2-D Array of doubles)*: The geocentric position X,Y,Z in meter of the satellite.
GPSvel	*(2-D Array of doubles)*: The geocentric velocity $\dot{X}$, $\dot{Y}$, $\dot{Z}$ in meter per second of the satellite.
SunPos	*(2-D Array of doubles)*: The geocentric position of the Sun in meter.
MoonPos	*(2-D Array of doubles)*: The geocentric position of the Moon in meter.
SunZD	*(Array of doubles)*: The solar zenith angle in degrees.
Vgeo	*(Array of doubles)*: The velocity of the satellite with respect to the Earth in meter per second.
Tcal	*(Array of doubles)*: The temperature in Kelvin of the calibration load.
Trec	*(Array of doubles)*: The mean value of the receiver nosie temperature in Kelvin used during the intensity calibration.
SBpath	*(Array of doubles)*: The path length in meter of the SSB diplexer.
AttitudeVersion	*(Array of integers)*: The version number of the attitude reconstruction software (SODA) used at SSC during production of attitiude files.

FreqRes	*(Array of doubles)*: The spacing in Hz between neighbouring channels for this spectrum.
FreqCal	*(2-D Array of doubles)*: These are the four local oscillator frequencies of the SSB modules.
IntTime	*(Array of doubles)*: The integration time in seconds, i.e. the duration of this observation.
EffTime	*(Array of doubles)*: The effective integration time in seconds, i.e. you will get the noise level in this spectrum by using this time and the receiver noise temperature from above and the usual radiometer formula: `dT = Trec/sqrt(df * EffTime)` where `df` is the bandwidth (FreqRes) of the spectrometer.
Channels	*(Array of integers)*: The number of channels in this spectrum.
FreqMode	*(Array of integers)*: Frequency mode applied.
TSpill	*(Array of doubles)*: Estimated Tspill in Kelvin.
ScanID	*(Array of integers)*: satellite time word scan identifier.
Apodization	*(Array of integers)*: The "channel response" filtering technique applied. 1 = Hanning smoothing
Frequency	This information can be used to create frequencys grid for the spectra, and consists of four fields: **LOFreq**: *(Array of doubles)*: Local oscillator frequency in Hz in the rest frame of the observed object, i.e Doppler corrected. **AppliedDopplerCorr**: *(Array of doubles)* The applied Doppler correction in Hz. **IFreqGrid**: *(Array of doubles)*: The frequency grid can be obtained by `frequency = LOFreq + IFreqGrid` . **SubBandIndex**: *(2-D Array of integers)*: The SubBandIndex can be used to identify from which sub-band a given channel belongs to. An example SubBandIndex array is [[-1, -1, 420, 509, 111, 1, 310, 200], [-1, -1, 508, 618, 199, 110, 419, 309]]. The first and second row indicate the start and end positions, respectively, of the eight sub-bands in the frequency sorted spectrum. The first and second index in these rows corresponds to SubBand 1 and 2, and so on. E.g sub-band 3 data can be found between index 420 to 508. -1 indicates that data from this band is not used. **ChannelsID**: *(Array of integers)*: Channel identifier describes the location of the sorted channels in the original unsorted spectra.

ZeroLagVar	*(2-D Array of doubles)*: Zerolag variation of the surrounding reference measurements for all sub-bands. `ZeroLagVar = abs(diff(ZeroLag))/mean(ZeroLag)` [%] ZeroLag is the measured coefficient of the first channel of the auto-correlator, and is proportional to the total power of the band.

Table 3.3: Odin/SMR PTZ data format. Example URL: http://malachite.rss.chalmers.se/rest_api/v4/ptz/2015-01-03/AC1/2/7002887494

Variable	Description
Pressure	*(Array of doubles)*: Pressure vector ([Pa]).
Temperature	*(Array of doubles)*: Temperature vector([K]).
Altitude	*(Array of doubles)*: Altitude vector([m]).
Latitude	*Double*: Latitude of PTZ data.
Longitude	*Double*: Longitude of PTZ data.
MJD	*Double*: Modified Julian Date of PTZ data.

Table 3.4: Odin/SMR *a priori* data format. Example URL: http://malachite.rss.chalmers.se/rest_api/v4/apriori/O3/2015-01-03/AC1/2/7002887494/

Variable	Description
Pressure	*(Array of doubles)*: Pressure vector([Pa]).
VMR	*(Array of doubles)*: Climatology volume mixing ratio vector [−] of the species.
Species	*(String)*: description of species, i.e. one of 'BrO', 'Cl2O2', 'CO', 'HCl', 'HO2', 'NO2', 'OCS', 'C2H2', 'ClO', 'H2CO', 'HCN', 'HOBr', 'NO', 'OH', 'C2H6', 'ClONO2', 'H2O2', 'HCOOH', 'HOCl', 'O2', 'SF6', 'CH3Cl', 'ClOOCl', 'H2O', 'HF', 'N2', 'O3', 'SO2', 'CH3CN', 'CO2', 'H2S', 'HI', 'N2O', 'OBrO', 'CH4', 'COF2', 'HBr', 'HNO3', 'NH3', or 'OClO'.

Quality flags

The Quality variable of an Odin/SMR Level1B structure is a scalar value. The value is determined from a quality control of both scan variables and the individual spectrum. Each test performed (see Table 3.5) is related to a unique scalar value and the Quality variable is the sum of the values of tests that were not passed. Thus, a spectrum with a Quality value of 0 is most reliable.

The most common situation is that most spectra in a given scan has a Quality value of 0, and a few spectra has a higher Quality value. In particular, the first and last spectrum of a scan tend to be more unreliable (Quality=0x0080). Many scan also contain one spectrum with a Quality=0x0100 since it is common that integration times changes during a scan, i.e. the spectra of the upper part of the scan has a greater integration time than spectra in the lower part of the scan. A spectrum with Quality 0x0080 or 0x0100 does not necessarily need to be corrupt, but the probability that it is corrupt is high. If the spectrum also failed to pass other tests it is corrupt.

The radiometric noise of the spectra of a scan is estimated as decribed in Sect. 2.3 (and reported as an effective integration time (EffTime)). This estimate does not contain the broadband noise (due to gain variation). The scan data contains the variable ZeroLagVar which can be seen as an estimate of the broadband gain variation (ZeroLagVar$\approx \frac{\Delta g}{g}$ [%]) of the two surrounding references of a target spectrum. If the ZeroLagVar is above ∼0.25 for a given sub-band than it is likely that data from this band has a large broadband offset.

Table 3.5: Description of the Odin/SMR Quality variable.

Test	Description	Value
check of Tspill	outside of valid range (3–12 K)	0x0001
check of Trec	outside of valid range (2000–4000 K)	0x0002
check of Noise	outside of valid range. Valid range is 0.5–6 K	0x0004
check of Scanning	tangent altitude is not decreasing or increasing as expected	0x0008
check of nr of Spectra	the scan consists of less than five spectra	0x0010
check of Tb	outside of valid range (-15 – 280 K)	0x0020
check of Tint	integration time is outside valid range. Valid range is 0.85 ± 0.01 s , 1.85 ± 0.01 s, or 3.85 ± 0.01 s	0x0040
check of References 1	atmospheric spectrum is not collected between two sky beam 1 references	0x0080
check of References 2	surrounding references have different integration times	0x0100
check of Moon hit	the moon is in the main beam	0x0200

Summary

Some key issues that should be considered when examining or applying Odin/SMR Level1B data:

- Odin/SMR can perform observations in a number of different frequency bands, mainly within the $486 - 504\,\text{GHz}$ and $541 - 581\,\text{GHz}$ regions. In practise, two or three frequency bands are measured simultaneously. For a given day, several observation modes can be applied, and hence it is rather complicated to describe the time-sharing in a comprehensive way.

- Calibrated spectra are expressed in terms of Rayleigh–Jeans brightness temperature.

- Odin/SMR spectra contain a significant amount of broadband noise, due to rapid gain fluctuations, in addition to radiometric noise.

Bibliography

U. Frisk, M. Hagström, J. Ala-Laurinaho, S. Andersson, J-C Berges, J-P Chabaud, M. Dahlgren, A. Emrich, H-G Florén, G. Florin, M. Fredrixon, T. Gaier, R. Haas, T. Hirvonen, Å. Hjalmarsson, B. Jakobsson, P. Jukkala, P-S Kildal, E. Kollberg, J. Lassing, A. Lecacheux, P. Lehikoinen, A. Lehto, J. Mallat, C. Marty, D. Michet, J. Narbonne, M. Nexon, M. Olberg, A. O. H. Olofsson, G. Olofsson, A. Origné, M. Petersson, P. Piironen, R. Pons, D. Pouliquen, I. Ristorcelli, C. Rosolen, G. Rouaix, A.V. Räisänen, G. Serra, F. Sjöberg, L. Stenmark, S. Torchinsky, J. Tuovinen, C. Ullberg, E. Vinterhav, N. Wadefalk, H. Zirath, P. Zimmermann, and R. Zimmermann. The Odin satellite I. Radiometer design and test. *A&A*, 402(3):L27–L34, 2003. doi: http://dx.doi.org/10.1051/0004-6361:20030335.

R. F. Jarnot, H. M. Pickett, and M. J. Schwartz. *EOS MLS Level 1 Data Processing Algorithm Theoretical Basis*. Number D-15210. 2004.

D. Murtagh, U. Frisk, F. Merino, M. Ridal, A. Jonsson, J. Stegman, G. Witt, P. Eriksson, C. Jiménez, G. Megie, J. de La Noë, P. Ricaud, P. Baron, J. R. Pardo, A. Hauchcorne, E. J. Llewellyn, D. A. Degenstein, R. L. Gattinger, N. D. Lloyd, W. F. J. Evans, I. C. McDade, C.S. Haley, C. Sioris, C. von Savigny, B. H. Solheim, J. C. McConnell, K. Strong, E. H. Richardson, G. W. Leppelmeier, E. Kyrölä, H. Auvinen, and L. Oikarinen. An overview of the Odin atmospheric mission. *Can. J. Phys.*, 80:309–319, 2002.

M. Olberg, U. Frisk, A. Lecacheux, A. O. H. Olofsson, P. Baron, P. Bergman, G. Florin, Å. Hjalmarson, B. Larsson, D. Murtagh, G. Olofsson, L. Pagani, A Sandqvist, D. Teyssier, S. A. Torchinsky, and K. Volk. The Odin satellite II. Radiometer data processing and calibration. *A&A*, 402(3):L35–L38, 2003. doi: DOI:10.1051/0004-6361:20030336.

Observation modes

Table A.1: Odin/SMR operational modes in aeronomy for AC1 and AC2 and the sub-mm frontends (FM = frequency mode)

Backend	Frontend	LO freq [GHz]	Source mode	FM
AC1	495 A2	492.750	Transport	23
		499.698	Transport	25
	549 A1	548.502	Stratospheric	2
		553.050	Water isotope	19
		547.752	Water isotope	21
		553.302	Transport	23
	555 B2	553.298	Summer mesosphere	13
	572 B1	572.762	Transport	24
AC2	495 A2	497.880	Stratospheric	1
		492.750	Water isoptope	8
		494.750	Water isotope	17
		499.698	Transport	25
	572 B1	572.762	Summer mesosphere	14
		572.964	Transport	22

Table A.2: Odin/SMR frontend and backend frequency specification for modes that are measured during part of the summer (when only backend AC2 is used, which is the case for 2013 and onwards). These modes are normally measured by backend AC1 (e.g. FM 102 and FM 2, FM 119 and FM 19, FM 121 and FM 21, and FM 113 and 13, are all identical except the Backend used).

Backend	Frontend	LO freq [GHz]	Source mode	FM
AC2	549 A1	548.502	Stratospheric	102
		553.050	Water isotope	119
		547.752	Water isotope	121
	555 B2	553.298	Summer mesosphere	113

Table A.3: Odin/SMR frontend and backend frequency specification

FM	SMR mode	LO Freq. [GHz]	Freq. Range [GHz]	Species	Name / ID
01	s1a or sc1a	497.880	501.180–501.580	ClO, O_3, N_2O	SM-AC2a / 01
			501.980–502.380		SM-AC2b / 02
					SM-AC2ab / 29
02	s1a	548.502	544.102–544.902	HNO_3 , O_3	SM-AC1e / 03
08	w3a or w5a	492.750	488.950–489.350	$H_2^{18}O$, O_3,$H_2^{16}O$	IM-AC2a / 13
			488.350–488.750		IM-AC2b / 14
					IM-AC2ab / 30
17	w4a or w5b	494.250	489.950–490.750	HDO, 18_3^O	IM-AC2c / 21
19	w3a or w4a	553.050	556.550–557.350	H_2O, O_3	IM-AC1c / 22
21	w5a or w5b	547.752	551.152–551.552	NO, O_3, $H_2^{17}O$	IM-AC1de / 31
			551.752–552.152		
13	sm1a	553.298	556.598–557.398	$H_2^{16}O$, O_3	HM-AC1c / 19
14	sm1a	572.762	576.062–576.862	CO, O_3	HM-AC2c /20
22	co1a	572.964	576.254–576.654	CO, O_3, HO_2,$^{18}O_3$	HM-AC2ab / 32
			577.069–577.469		
23	co1a	492.750	488.350–488.750	$H_2^{16}0$, O_3	HM-AC1d / 33
		553.302	556.702–557.102		HM-AC1e / 34
24	sc1a	572.762	576.062–576.862	CO, O_3	HM-AC1e / 35
25	ut1a	499.698	502.998–504.198	$H_2^{16}O$, O_3	TM-ACs1 / 36

Time series of Level0 and Level1B data

Figure B.1 displays trends in level0/level1b parameters, including brightness temperature from stratospheric FM 1 and 2. Tb501w and Tb544w represent the average Tb within frequency bands around 501.2 and 544.4 GHz, respectively. Tb544line represents Tb around the strong ozone transition around 544.8 GHz. The figure only contains data from measurements that correspond to low tangent points (below 9 km) within the tropical region. A negative trend (measurements being colder with time) can be noted in the figure. The trend is greater for the 544 GHz band. This trend is not completely understood.
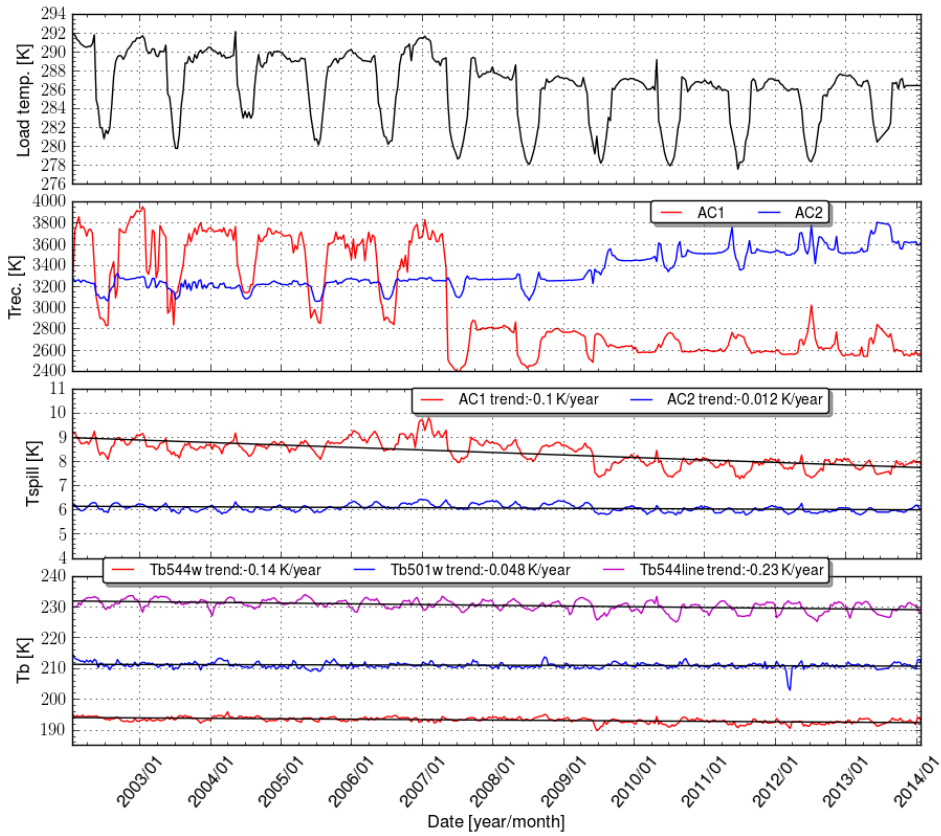
Figure B.1: Trends in level0/level1b parameters. Upper panel shows the internal load temperature, second panel receiver noise temperature, third panel shows T_{sp} temperature, and bottom panel shows calibrated brightness temperatures from stratospheric FM1 and FM2 measurements (see text for details) during 2002–2014. Each datapoint in the figure represents a 10 day average.

Comparison of data from different calibration versions

The current operational Odin/SMR level2 processing at Chalmers is based on Level1B calibration version 7 (L1B-v7) data. The L1B-v7 is known to have some issues, and a new calibration version (L1B-v8) has been developed. The L1B-v8 builds upon the the L1B-v7 algorithm, but some changes have been applied, with the natural aim to reduce these issues.

- L1B-v7 algorithm is orbit based, in the sense that some calibration parameters (T_{rec} and T_{sp}) are common for all scans from a given orbit and frequency mode. L1B-v8 is scan based, as desribed in Chapter 2.

- L1B-v8 is more strict when it comes to selecting which reference measurements to use. The movement of an internal mirror can affect the reference measurements when switching towards the internal load, with a negative impact on final atmospheric spectra. A more adequate and standardised removal of spectra that are possibly affected by the mirror movement is performed in L1B-v8 compared to in L1B-v7.

- L1B-v8 also make sures that the instruments settings are the identical for all spectra that will be calibrated with shared parameters. For most data this was not issue with L1B-v7, as the instruments settings are most often only changed when switching observation mode.

- L1B-v8 aims for removing ripple seen in calibrated measurements in the upper part of the scan (see Figure C.1).
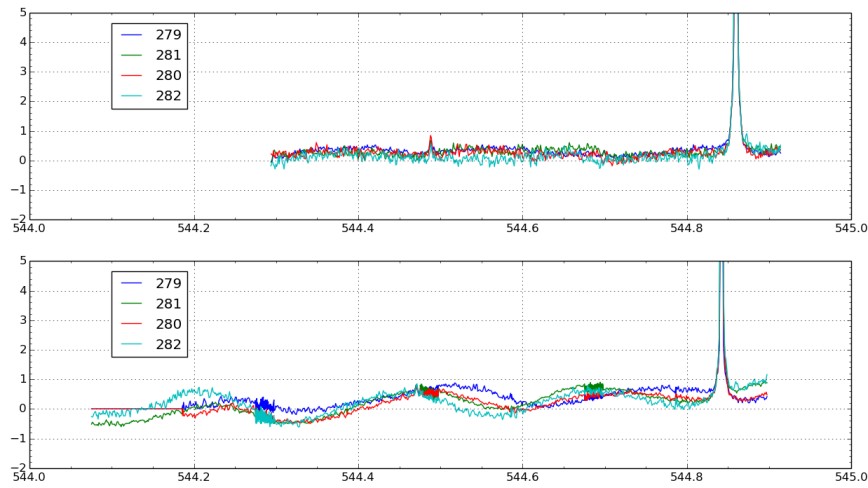
Figure C.1: Upper panel shows averages of calibrated spectra (verison 8) from measurements with tangent altitudes above 60 km for one of the most used frequency modes (FM 2) for May 2009. The colorcoding/legend corresponds to the ambient temperature or load temperature. The lower panel shows corresponding data, but for calibration version 7 data.

Frequency corrections for CO

Odin/SMR measures CO at an emission line resulting from the $J = 5 \rightarrow 4$ rotational transition, with a center frequency at 576.268 GHz. This is measured together with an O_3 line at a frequency band of 576.254 - 576.654 GHz in a stratospheric/mesospheric scan, corresponding to altitudes between roughly 7 km and 110 km. An example of such a measurement is shown in Figure D.1.
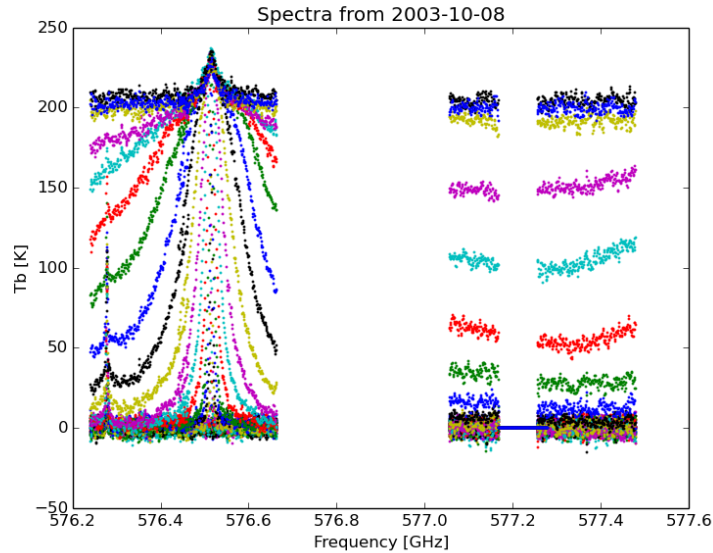
Figure D.1: Brightness temperature spectra for altitudes ranging from 7 km to 110 km at the frequency band [576.254 - 576.654, 577.069 - 577.469] GHz (Odin/SMR frequency mode 22). The CO line corresponds to the first peak at the lower frequency and the O_3 line measured simultaneously is shown at the higher frequency.

The B1 frontend of Odin/SMR is used for all measurements of this CO line, which sets the frequency range between 563 GHz and 581 GHz. The Phase-Lock Loop (PLL) in the Odin/SMR instrument (see Figure 1.1) controls the fine tuning of the frequencies to use for an observation, within the range set by the frontend. Due to a failure in the PLL component of B1, the local oscillator (LO) frequency is offset from the demanded frequency. For a year long period between 2003-10-08 and 2004-10-08, the PLL used for CO measurements was functioning, but all other observations were affected by this PPL malfunction. This has resulted in a frequency shift that varies from one scan to another in such a way that the lines can either be moved in a positive or negative direction, or lines might be missed completely in the observation. Examples of different shifts are shown in

Figures D.2 and D.3. In Figure D.3 it can be seen that there are measurements where CO is not included in the spectra, which means that no data can be recovered.
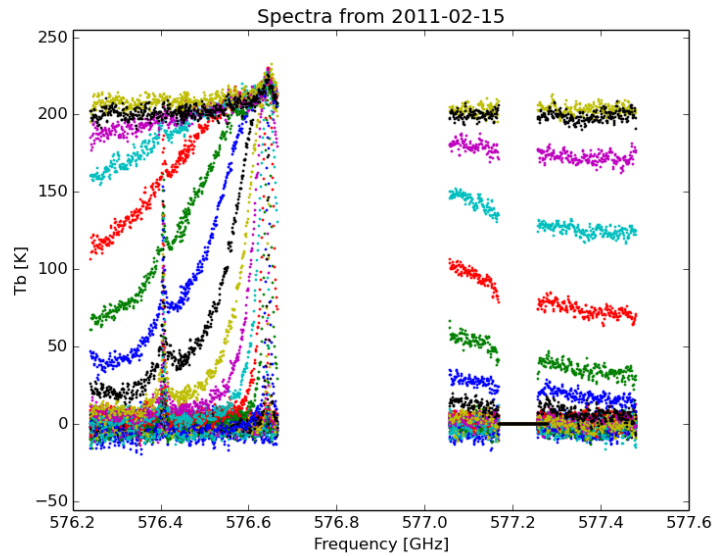

Figure D.2: Brightness temperature spectra measured 2011-02-15, showing an example of a frequency shift where both species are still included.
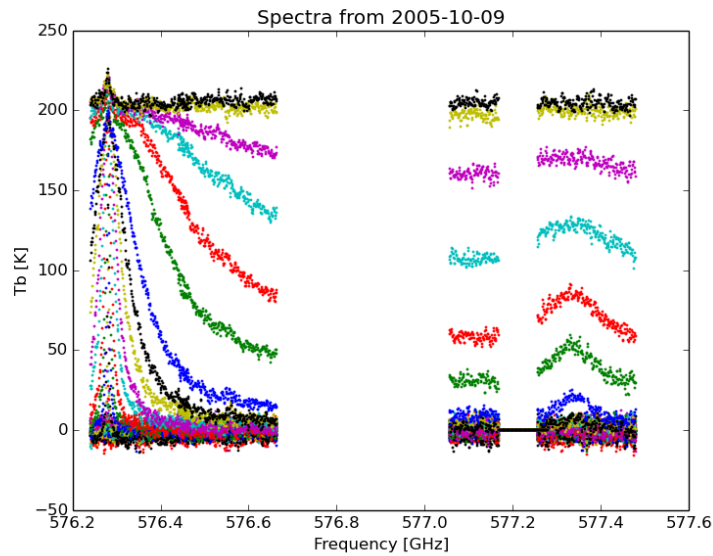

Figure D.3: Brightness temperature spectra measured 2005-10-09, showing an example of a frequency shift where only the O_3 line is included.

In order to correct the frequency shift, an algorithm has been developed and added to the retrieval process of CO. Accurate frequency calibration is done in the algorithm by comparing the observed center frequency and the theoretical center frequency of 576.268 GHz of the CO line, using the difference to shift the spectra. In order to do this, the CO line

must first be located by the algorithm and distinguished from the O_3 line. The distinction is performed by observing the slope of the brightness temperature measurements between altitudes of 40 km and 60 km, as is illustrated in Figure D.4.
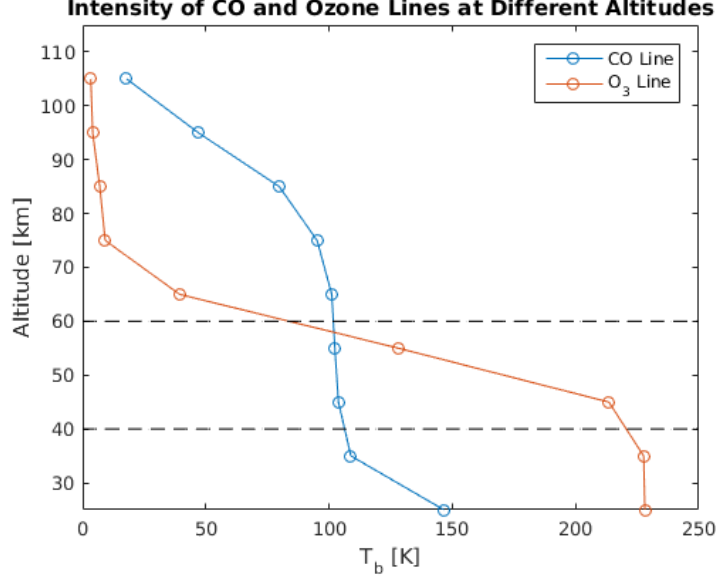

Figure D.4: Brightness temperatures, corresponding to the maximum of the peak of CO and O_3, at different altitudes. The values are averaged over observations between 2003-10-08 and 2004-10-08, when the PLL component was functioning. A clear difference between the red and blue curve can be observed in the slope between 40 km and 60 km.

A linear fit of the measured brightness temperatures with respect to altitude is performed between 40 km and 60 km. As can be observed in Figure D.5, there is a clear separation between the slopes of the different curves. If the obtained slope is larger than a cutoff chosen at -0.0045 K/m, the line is identified as CO and the algorithm will continue to the next step of the correction. If no line is found in the measured spectra or if only the O_3 line is found, the scan is marked as unuseful and no additional corrections are made.

Once the observed CO line has been located, the corresponding observed center frequency is determined. In order to do this, a Gaussian fit according to equation (D.1) is applied to the measured data, where b represents the center frequency. The difference between the obtained center frequency b and the theoretical center frequency of 576.268 GHz is then applied to the local oscillator frequency of the radiometer, which means that all frequency values of the spectra are adjusted accordingly. The Gaussian fit and the correction are illustrated in Figure D.6.

$$f(x) = a \cdot \exp\left(-\left(\frac{x-b}{c}\right)^2\right) \tag{D.1}$$

The amount of measurements that have been made, each year from 2001 until 2015, is shown in Figure D.7, together with the number of measurements that could be recovered and the amount that could not. Table D.1 shows the number of measurements that is affected and the number that is unaffected by the PLL malfunction, together with the precentage of the measurements that could be recovered in total and for each year between 2001 and 2015.
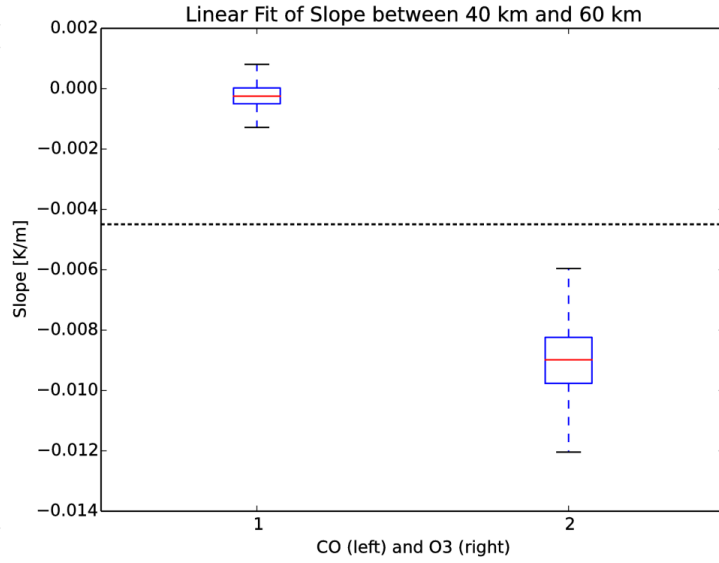
Figure D.5: The slope of a linear fit of the brightness temperature between altitudes of 40 km and 60 km for CO and O_3. The data includes all observations between 2003-10-08 and 2004-10-08, when the PLL component was functioning. A cutoff between the two species can be observed around -0.0045 K/m.
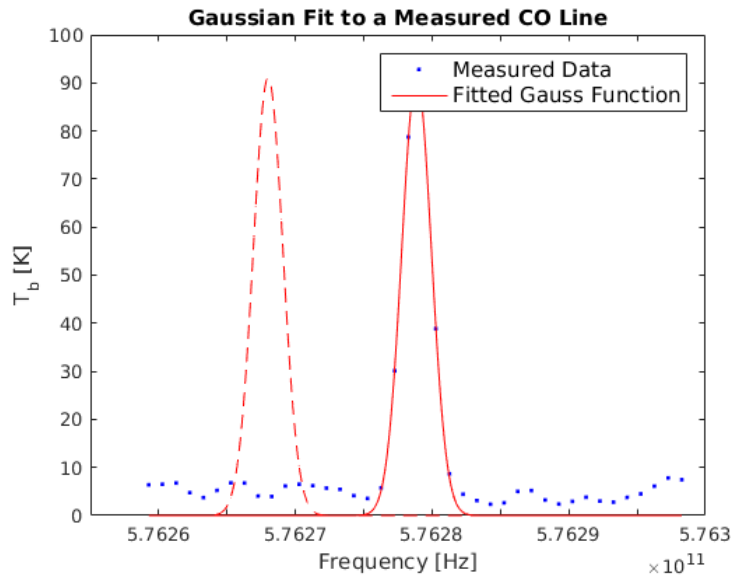

Figure D.6: An example of measured brightness temperatures for CO at a single altitude, together with a Gaussian fit of the values. The dashed red line shows the theoretical center frequency, where the line is shifted to.
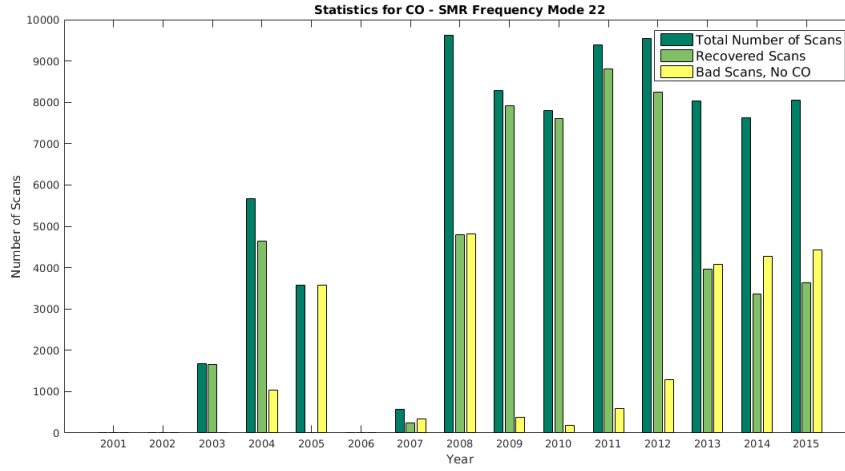
Figure D.7: The amount of available data for CO from frequency mode 22 of Odin/SMR calculated for each year ranging from the start in 2001 until 2015.

Table D.1: The number of measurements that is affected and unaffected by the PLL malfunction, together with the precentage of the measurements that could be recovered. The data is displayed for each year from 2001 to 2015 and in total.

Year	# Unaffected	# Affected	Recovered [%]
2001	0	0	0
2002	0	0	0
2003	1670	0	100
2004	4687	988	82
2005	0	3570	0
2006	0	0	0
2007	0	569	41
2008	0	9623	49
2009	0	8282	95
2010	0	7797	97
2011	0	9392	93
2012	0	9550	86
2013	0	8036	49
2014	0	7634	44
2015	0	8060	45
Total	6357	73501	68